A railway HIL system for the safety on board subsystem testing activities: controller robustness analysis

B. Allotta[1], F. Cavaliere [2], R. Conti[1], E. Meli[1], L. Pugi[1], A. Ridolfi [1]

[1] University of Florence, Department of Industrial Engineering,
via Santa Marta 3, Florence, Italy. roberto.conti@unifi.it

[2] Laboratorio Materiale Rotabile (LMR), Italcertifer S.p.A.,
Florence, Italy.

Abstract

In recent years, the employment of high speed railway vehicle for passenger transport in the European countries is notably increased and the travelling speeds are passed the limit of 350 km/h, introducing important problems in the safety fields. Therefore, accurate testing activities on the influence between wheel-rail adhesion conditions and the safety on board subsystems (such as odometry algorithms, wheel slide protection devices (WSP) and anti-skid devices) have to be performed. Usually, the testing activities consist of complex experimental tests (required by the regulation in force on the safety on board subsystems) mainly performed by means of on-track tests. Moreover, the technological improvements, the integration of different on board subsystems and their mutual interaction have to be carefully evaluated. The main problems related to the on-track tests are the high economic investments and the speed limitations (the maximum speed limit for most of the testing circuits is often limited to 200 km/h) which may negatively affect the development and the calibration of the high speed devices. Thanks to the economic investment of several national and academic institutions, a railway research and homologation center ("Centro di Dinamica Sperimentale (CDSO)") has been recently inaugurated in Firenze Osmannoro (Florence, Italy). One of the most advanced testing equipment of CDSO is an innovative full scale roller rig with the aim of reproducing degraded adhesion conditions and testing both traction and braking equipments at high speed (over 350 km/h). Innovative features, comparing with conventional roller rigs, are related both to the roller rig performances and to the degraded adhesion simulation strategies. In particular, the macro-sliding are notably reduced in order to avoid a significant wear or damage of the rolling surfaces. In this work, the authors will analyze the dynamical behaviour of the roller rig in terms of Hardware In the Loop (HIL) performance, stability and controller robustness when degraded adhesion conditions occur. The reproduced tests in the HIL simulation model are performed only in braking phases.

Keywords: *Multibody model of railway vehicles, Hardware In the Loop, Degraded adhesion.*

1 Introduction

In high speed trains, the development and the testing phase of the on-board subsystems represent a crucial part of the design of the railway vehicle. Nowadays, the integration and the mutual interaction between the traction and the braking on-board subsystems are rapidly increasing. These aspects have to be analysed and investigated in order to prevent dangerous situations.

Fullscale roller-rigs are usually used to test traction and braking performances of complete railway vehicles [1], [6]. Modern traction and braking systems are equipped with specific on-board subsystems, respectively named antiskid (for traction) and Wheel Slide Protection (WSP) system, for braking; such subsystems are able to correct the longitudinal efforts applied to the axles to prevent excessive sliding among wheels and rail. It is important to limit the slidings because they may seriously damage the rolling surfaces, negatively affecting braking and traction performances and consequently the safety and traffic management. The simulation of degraded adhesion conditions is sometimes performed on roller-rigs to identify the behaviour of the vehicle and of the wear [5],[6]. However the testing of braking and traction subsystems on roller-rigs (considering degraded adhesion conditions) is still limited to few applications, since sliding between roller and wheel produces the wear of the rolling surfaces; this event is not acceptable because of the corresponding effect on maintenance costs of the rig (rollers have to be turned or substituted) and the potentially dangerous working conditions arising from the change of contact conditions due to wear.

In previous research activity [5] the authors have proposed a feasibility analysis of a HIL architecture able to reproduce

on the rollers a virtual adhesion pattern (especially, degraded adhesion conditions) performing a simulation of mechanical impedance: roller motors are controlled in order to reproduce the same tangential efforts (exchanged between the wheelsets and the rail) calculated by a reference wheel-rail degraded adhesion model. Since the real adhesion factor between the roller and the wheel is far higher than the simulated one, negligible sliding occurs between them. The main limitations of this work are related to the many simplifying assumptions: in particular, all the models are completely 2D (also for the contact model between roller and wheel [5]) and the wheel-rail adhesion model is very simple and not validated by any experimental results.
According to this research activity, Trenitalia has recently built the proposed HIL system in the railway research center "Centro di Dinamica Sperimentale di Firenze-Osmannoro" (CDSO); this HIL architecture consists of a fullscale roller-rig and a virtual railway vehicle model where the desired adhesion conditions are completely simulated; the controller is then able to reproduce these conditions on the roller-rig. Recently, Italcertifer S.p.A. (the owner of the CDSO) and Trenitalia S.p.A., in collaboration with several academic institutes, are performing the pre-testing activity on the HIL system installed in the CDSO in order to evaluate the real characteristics and performances of this complex mechatronic system. Therefore, the authors, to better study and to support this pre-testing activity, have developed a new complete model characterized by innovative features and based on the real electro-mechanical characteristics of the devices. The main innovative aspects developed in the model (compared with the feasibility analysis realized in [5]) can be summarized: the development of 3D multibody models of the roller-rig and of the railway vehicle (the data of which are provided by Trenitalia and Italcertifer); the implementation of innovative control laws to increase the stability and the robustness of the 3D model and finally, an innovative 2D adhesion model used in the virtual railway vehicle model and developed to simulate degraded adhesion conditions.
The study of the performance and the controller robustness (with regard to different physical and geometrical parameters) represents an important topic for this kind of applications; moreover, through this research activity it will be possible to pre-analyze the interactions between the vehicle and the roller-rig, highlighting the main critical situations during a real test. In this way, the performance and robustness analysis assumes a dual aspect because the performed analysis will be used to evaluate the real HIL performance and to define unsafely situations for the personnel and the equipments.

2 CDSO HIL system: general architecture

The general architecture of the HIL system is schematically shown in the block diagram of Fig. 1.

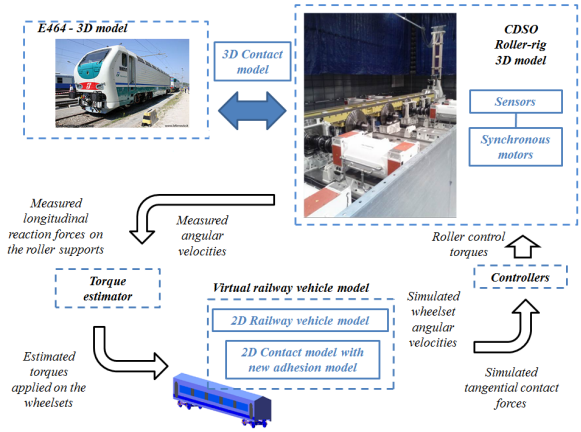

Figure 1. General architecture of the CDSO HIL system

The following main blocks can be identified in the scheme:

1. ***Roller-rig model***: the roller-rig model is based on the technical data provided by Italcertifer [2] during the collaboration in order to define the real characteristics of the CDSO roller-rig in terms of actuation system and mechanical components. The system consists of a 3D multibody model linked with the roller motor models. The roller motors are synchronous machines especially developed for this advanced application with an indirect vectorial controller.
2. ***Vehicle model***: the considered vehicle model proposed by Italcertifer for the real pre-testing activity is the E464 locomotive and it is described through a parametric 3D multibody model. The model is characterized by two suspension systems (primary and secondary stages) and several non-linear elements (such as roll-bar, anti-yaw, etc.) implemented according to the technical handbook of the E464 vehicle [3].

3. ***Virtual railway vehicle model***: it represents the model of the vehicle used to simulate the locomotive behaviour on the rails in different adhesion conditions and therefore has to be designed for a real-time implementation (a 2D multibody model is used for the longitudinal dynamics of the vehicle). The implemented 2D adhesion model (especially developed by the authors for degraded adhesion simulations) presents several innovative characteristics [4] because it is based on a new energetic criterion.

4. ***Controllers***: the controller model should reproduce on the roller rig the same dynamical behaviour of the virtual train model, in terms of wheel angular velocities and vehicle motor torques [5], without macro-sliding between wheels and rollers. Due to the HIL system non-linearities a sliding mode approach is adopted in the controller.

5. ***Estimator***: this block is necessary to evaluate the real torque applied by the vehicle motors on the wheels, because the torque cannot be directly measured. This part includes the simulation of the sensors installed on the CDSO roller-rig such as absolute encoder and a 3-axial load cell.

The CDSO HIL system has been implemented in the Matlab - Simulink® environment; particularly, the multibody model has been implemented in the Simulink® toolbox SimMechanics.

3 The Hardware In the Loop Approach

3.1 The Test-rig Model

The inputs of the whole test-rig model are the 8 roller control torques u evaluated by the controllers to reproduce on the test-rig the same dynamical behaviour of the virtual railway model. The outputs are the 8 roller angular velocities ω_r and the longitudinal reaction forces T_{mis} measured on the roller supports.

3.1.1 The Vehicle Model

The considered railway vehicle is the E464; its geometrical and physical characteristics are provided by Trenitalia [3]. The wagon consists of one carbody, two bogie frames, eight axleboxes and four wheelsets. The E464 vehicle has a two-stage suspension system: the primary suspension, including springs, dampers and axlebox bushings, connects the bogie frames to the four axleboxes while the secondary suspension, including springs, dampers, lateral bump-stops, anti-roll bar and traction rod, connects the carbody to the bogie frames. The multibody vehicle model takes into account all the degrees of freedom (DOFs) of system bodies. Both the primary suspensions and the secondary ones have been modelled through 3D visco-elastic force elements able to describe all the main non-linearities of the system.
The inputs of the model are the 4 wheelset torques C_s modulated by the on board WSP and the contact forces calculated by the contact model, while the outputs are the kinematic wheelset variables transmitted to the contact model, the 4 original torques C (without the on board WSP modulation) and the 4 wheelset angular velocities ω_w. These last two outputs are not accessible by the HIL system. The WSP device installed on the E464 vehicle [3] allows the control of the torques applied to the wheelsets, to prevent macro-sliding during the braking phase. The WSP inputs are the braking torques C and the wheelset velocities ω_w while the outputs are the modulated braking torques C_s. The WSP system working principle can be divided into three different tasks: the evaluation of the reference vehicle velocity V_{ref} and acceleration a_{ref} based on the wheelset angular velocities ω_w and accelerations $\dot{\omega}_w$; the computation of the logical sliding state $state_{WSP}$ (equal to 1 if sliding occurs and 0 otherwise)and the consequent torque modulation, through a speed and an accelerometric criterion and by means of a suitable logical table; the periodic braking release to bring back the perceived adhesion coefficient to the original value (often used when degraded adhesion conditions are very persistent and the WSP logic tends to drift).

3.1.2 The Roller-rig Model

The 3D multibody model of the roller-rig (see Fig. 1 and Tab. 1) consists of 8 rollers with a particular roller profile able to exactly reproduce the UIC60 rail pattern with different laying angles α_p. The railway vehicle is axially constrained on the rollers using two axial links (front and rear) modelled by means of 3D force elements with linear stiffness and damping. The inputs of the test-rig model are the 8 torques u evaluated by the controllers and the contact forces calculated by the contact model; the outputs are the roller angular velocities ω_r, the longitudinal reaction forces T_{mis} measured on the roller supports and the kinematic wheelset variables transmitted to the contact model. The roller-rig actuation system consists of 8 synchronous motors, especially designed and developed in cooperation with SICME [2] for this kind of application. The HIL architecture includes a direct-drive connection between the roller and the electrical machine. The synchronous motors have high efficiency associated with high torque density and flux weakening capability. Furthermore, to reach the dynamical and robustness performances required by the railway full-scale roller-rig, the motors are designed

Table 1. Main characteristics of the roller-rig system and of the wheelsets

Parameter	Units	Value
Roller radius r_r	m	0.725
Roller mass m_r	kg	2980
Roller inertia J_r	kgm^2	705
Wheelset radius r_w	m	0.445
Wheelset mass m_w	kg	1300
Wheelset inertia J_w	kgm^2	160
Motor nominal torque T_{nom}	Nm	38500
Motor maximum angular speed ω_{max}	rad/s	141
Motor inertia J_{mot}	kgm^2	200

with a multilayer-rotor characterized by a high saliency ratio and Interior Permanent Magnets (IPM). The IPM motors are controlled in real-time through vector control techniques; more particularly the vector control is a torque-controlled drive system in which the controller follows a desired torque. The main sensors installed on the roller-rig are the absolute encoders and the 3-axial load cells on the roller supports.

3.1.3 The Wheel-roller Contact Model

The 3D contact model evaluates the contact forces $\underline{N}_c$, $\underline{T}_c$ for all the 8 wheel-roller pairs starting from the kinematic variables of the wheelsets and of the rollers: their positions $\underline{G}_w$, $\underline{G}_r$, orientations $\underline{\Phi}_w$, $\underline{\Phi}_r$, velocities $\underline{v}_w$, $\underline{v}_r$ and angular velocities $\underline{\omega}_w$, $\underline{\omega}_r$ (see Fig. 2 (b)).
The contact model comprises three different steps. Firstly, all the contact points $\underline{P}_c$ of each wheel-roller pair are detected.

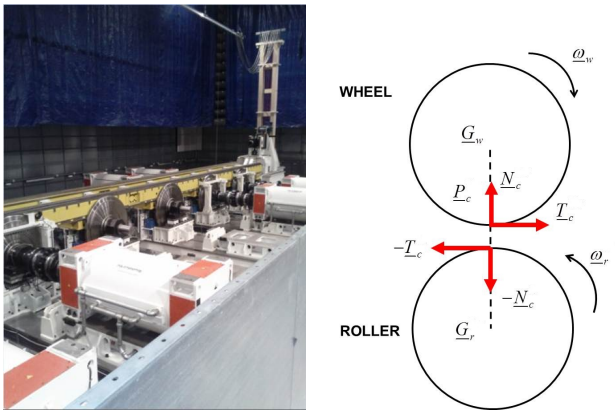

(a) (b)

Figure 2. (a) CDSO roller-rig (b) Wheel-roller contact model

Some innovative procedures have been recently developed by the authors [7], [9]; the new algorithms are based on the reduction of the algebraic contact problem dimension through exact analitical techniques. Secondly, the normal contact problem is solved through the Hertz theory to evaluate the normal contact forces $\underline{N}_c$. Finally, the solution of the tangential contact problem is performed by means of the Kalker-Polach theory to compute the tangential contact forces $\underline{T}_c$. The contact model guarantees high accuracy and numerical efficiency; this way, the model can be implemented directly online inside the whole test-rig model.

3.2 The Virtual Railway Vehicle Model

The virtual railway vehicle model simulates the dynamical behaviour of the railway vehicle during a braking phase under degraded adhesion conditions. The model, designed for a real-time implementation, is composed of two parts: the 2D vehicle model and the 2D adhesion model. The inputs are the 4 estimated torques $\widehat{C}_s$ to be applied to the wheelsets while the outputs are the 4 simulated tangential contact forces T_{sim} and the 4 simulated wheel angular velocities ω_{ws}.
The 2D vehicle model of the considered railway vehicle (E464 vehicle) is a simplified 2D multibody model of the longitudinal train dynamics (only 3 DOFs for each body are taken into account). The model consists of a carbody, two bogies and four wheelsets, held by the primary and secondary suspensions. Starting from the estimated torques $\widehat{C}_s$, the model evaluates the kinematic variables of the 4 wheelsets v_{ws}, ω_{ws} and the 4 normal contact forces N_{cs} to be passed to the

adhesion model and receives the 4 tangential contact forces T_{sim}.
The adhesion model has been especially developed to describe degraded adhesion conditions [4], [8] and calculates, for all the 4 wheelset-rail pair, the tangential contact forces T_{sim} starting from the wheelset kinematic variables v_{ws}, ω_{ws} and the normal contact forces N_{cs} (see Fig. 3).
The main phenomena characterising the degraded adhesion are the large sliding occurring at the contact interface and,

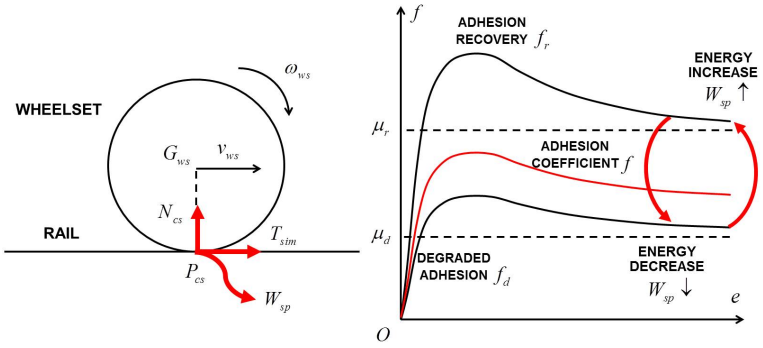

Figure 3. The adhesion model

consequently, the high energy dissipation. Such a dissipation causes a cleaning effect on the contact surfaces and finally an adhesion recovery due to the removal of the external contaminants. When the specific dissipated energy W_{sp} is low the cleaning effect is almost absent, the contaminant level h does not change and the adhesion coefficient f is equal to its original value f_d in degraded adhesion conditions f_d. As the energy W_{sp} increases, the cleaning effect increases too, the contaminant level h becomes thinner and the adhesion coefficient f raises. In the end, for large values of W_{sp}, all the contaminant is removed (h is null) and the adhesion coefficient f reaches its maximum value f_r; the adhesion recovery due to the removal of external contaminants is now completed. At the same time if the energy dissipation begins to decrease, due for example to a lower sliding, the reverse process occurs (see Fig. 3).
Since the contaminant level h and its characteristics are usually totally unknown, it is usefull trying to experimentally correlate the adhesion coefficient f directly with the specific dissipated energy W_{sp}:

$$W_{sp} = T_{sim} e = f N_{cs} e \quad f = \frac{T_{sim}}{N_{cs}} \tag{1}$$

where the creepage e is defined as

$$e = \frac{s}{v_{ws}} = \frac{v_{ws} - r_w \omega_{ws}}{v_{ws}}, \tag{2}$$

s is the sliding and r_w is the wheel radius. This way the specific dissipated energy W_{sp} can also be interpreted as the energy dissipated at the contact for unit of distance travelled by the railway vehicle.
To reproduce the qualitative trend previously described and to allow the adhesion coefficient to vary between the extreme values f_d and f_r, the following expression for f is proposed:

$$f = [1 - \lambda(W_{sp})] f_d + \lambda(W_{sp}) f_r \tag{3}$$

where $\lambda(W_{sp})$ is an unknown transition function between degraded adhesion and adhesion recovery while the adhesion levels f_d, f_r can be evaluated according to [4] as a function of e, N_{cs} and the track friction coefficients μ_d, μ_r (corresponding to degraded adhesion and full adhesion recovery, respectively). The function $\lambda(W_{sp})$ has to be positive and monotonous increasing; moreover the following boundary conditions are supposed to be verified: $\lambda(0) = 0$ and $\lambda(+\infty) = 1$.
This way, the authors suppose that the transition between degraded adhesion and adhesion recovery only depends on W_{sp}. This hypothesis is obviously only an approximation but, as it will be clearer in the next chapters, it well describes the adhesion behaviour. Initially, to catch the physical essence of the problem without introducing a large number of unmanageable and unmeasurable parameters, the authors have chosen the following simple expression for $\lambda(W_{sp})$:

$$\lambda(W_{sp}) = 1 - e^{-\tau W_{sp}} \tag{4}$$

where τ is now the only unknown parameter to be tuned on the base of the experimental data (in this case $\tau = 1.9 * 10^{-4}$m/J)[4]. Finally the tangential forces $T_{sim} = f N_{cs}$ can be evaluated starting from the adhesion coefficient f calculated by solving the non-linear equation 3 (see Eq. 1 for the definition of W_{sp}).

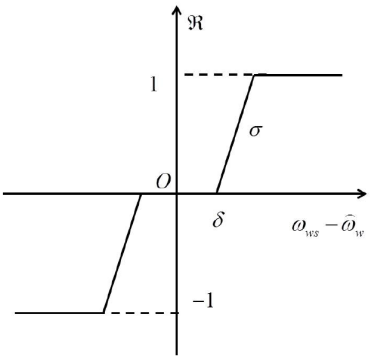

Figure 4. Discontinous control characteristics

3.3 The Controllers

The controller target has to be able to reproduce on the roller rig the dynamical behaviour of the virtual railway vehicle in terms of angular velocities ω_w and torque C_s. The controller architecture is the same explained in previous works [5] and [8] but for this innovative application a more stable and robust implementation is carried out. The inputs of the controller are the simulated tangential forces T_{sim}, the simulated wheel angular velocities ω_{ws}, the estimated wheel angular velocities $\widehat{\omega}_w$ and the estimated motor torques $\hat{C}_S$. The outputs are the eight control roller torques u_i (see Figure 1). The controller layout consists of 8-independent controller, one for each roller, in order to reproduce different adhesion conditions.
The control strategy consists in a sliding mode controller based on the dynamical equations of the roller rig; in this way, it is possible to reduce the disturbance effects in terms of non-linearity of the system and physical parameter uncertainties. These effects are stronger than the previous works (where only a 2D model is implemented) and are caused by the 3D modelling of the rollers and the wheelsets. The total control torque is defined as:

$$u_{tot} = u_{cont} + u_{disc} \tag{5}$$

where:

- u_{cont} is the continuous control part based on the dynamic model:

$$u_{cont} = \frac{R}{r_v}(\hat{C}_S(1 - \frac{J_B}{J_v}) + \frac{J_B}{J_v} T_{sim} r_v), \tag{6}$$

  in which J_B is the total moment of inertia of the roller and the simulated vehicle defined considering the wheel rotation axis

$$J_B = (J_v + J(\frac{r_v}{R})^2) \tag{7}$$

  (R is the roller radius), r_v is the wheel radius, J_v is the moment of inertia of the wheelset, J is the roller inertia moment;

- u_{disc} is the discontinuous control part related to the rejection of the parameter uncertainties that are much stronger in the 3D model (compared with a 2D model):

$$u_{disc} = k\Re(\omega_{ws} - \widehat{\omega}_w), \tag{8}$$

  where ω_{ws} represents the simulated angular velocity and $\widehat{\omega}_w$ is the estimated angular velocity. The discontinuous control is characterized by the gain k and the function $\Re$ shown in Figure 4; the parameters k, δ and σ have to be tuned.

3.4 The Torque Estimators

The estimators aim at evaluating the wheelset angular velocities $\widehat{\omega}_w$ and the torques applied to the wheelset $\widehat{C}_s$ starting from the roller angular velocities ω_r and the longitudinal reaction forces T_{mis} on the roller supports. Since the slidings between wheelset and rollers can be neglected, the following estimations approximately hold:

$$\hat{\omega}_w = -\frac{r_r}{r_w}\omega_r \quad \hat{\dot{\omega}}_w = -\frac{r_r}{r_w}\dot{\omega}_r \quad \hat{T}_c = T_{mis}. \tag{9}$$

Of course, the derivative operation $\frac{d}{dt}$ has to be robust, taking into account the numerical noise affecting ω_r. At this point, to estimate the motor torque applied to the wheelset, the estimator employes the simplified dynamical model of the wheelset:

$$\hat{C}_s = J_w \hat{\dot{\omega}}_w - \hat{T}_c r_w. \tag{10}$$

It is worth noting that, in this kind of applications, the estimators have to be necessarily simple because they are thought for a real-time implementation and, at the same time, the physical characteristics of the railway vehicle on the roller-rig are generally unknown.

4 Performance and robustness analysis

4.1 Nominal test

In this section the authors present the nominal tests in braking phase, used as reference in this article. These tests are performed on the E464 locomotor and they are used to test the performances of the safety on board subsystem model (Wheel Slide Protection WSP model for braking phase), ruled by the technical description in [2]. The main objective of this chapter is to analyze the performances and the robustness of the CDSO HIL architecture when degraded adhesion conditions are simulated.
The analysis defines a nominal situation where the vehicle and the CDSO roller-rig characteristics are completely standard (see the previous chapter for further details). The nominal conditions are: simulated adhesion coefficient $\mu_c = 0.08$, the maximum available adhesion coefficient $\mu_{rec} = 0.15$ and the initial speed $V_{init} = 80$ km/h.

Table 2. Nominal values of the physical and geometrical parameters

Requirement	Parameter	Value	Perturbed value
Constrain parameters			
DOF constraint		5 DOF	2 DOF
Constraint stiffness	k_c	10^8	$5*10^7$
Constraint damping	c_c	10^5	$5*10^4$
Initial z-displacement	z_{disp}	0 m	$\pm$0.1 m
Initial x-displacement	x_{disp}	0 m	0.01 m
Initial y-displacement	y_{disp}	0 m	0.002 m
Controller parameters			
Controller dead zone	δ	0.03	0.5
Controller gain	k	$2*10^4$	10^4
Controller slope	σ	10	1
Sensor parameters			
Torque estimator cut-off frequency	τ_t	1 kHz	100 Hz -500 Hz

In the nominal braking test, the braking phase starting from 80 km/h under degraded adhesion condition is simulated. The test parameters are the nominal value both of the E464 locomotor and of the CDSO roller-rig characteristics and are reported in Table 2. In the experimental on-track tests, the recovery adhesion effect is due to the contaminants destruction upon the rail by means of the dissipated power in the wheel-rail interface; the replication of this effect on the CDSO roller-rig is mainly caused by the innovative characteristics of the test rig and the 2D adhesion model (based on energetic criterion) implemented in the *Virtual railway vehicle model*.
In figure 5 (a), the behaviour of the adhesion coefficient is showed; it is interesting to observe the good agreement between the simulated adhesion coefficient μ_{sim} (coming from by the Virtual railway vehicle model), the estimated adhesion coefficient μ_{est} (coming from by the estimator model) and the measured one μ_{mis} (coming from by the ratio between the normal load and the tangential one in the roller-rig model); therefore, both the torque estimator and the controller part work very well. The initial value of the measured coefficient is coherent with good adhesion conditions ($\mu_{mis} = 0.3$) because at the beginning of the simulation, in the roller-rig, the adhesion coefficient is really high. After a transient, the controller is able to reduce the adhesion coefficient to the simulated one (in order to reproduce the same tangential efforts simulated by the virtual railway vehicle model). The recovery adhesion effect is really evident in this graphics: the final part of the graphic shows that the adhesion coefficient is near the nominal maximum value (near 0.15).
As regards both the torque estimation error e_c (Fig.5 (b)) and the angular speed error e_ω (Fig.6 (a)), it is possible to observe that the maximum values after the transient are really low; these effects prove the robustness of the control law and of the HIL architecture. The transients are completely rejected both in the initial part and in the recovery adhesion part (where adhesion coefficient begins to increase).

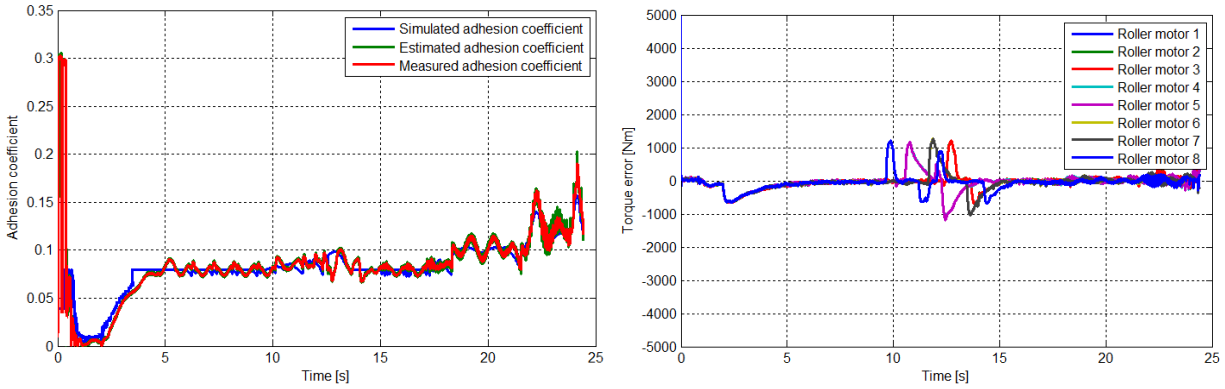

(a) (b)

Figure 5. (a) comparison among the simulated μ_{sim}, the estimated μ_{est} and the measured adhesion coefficient μ_{mis} for the I wheelset (b) torque estimation error e_c of the CDSO roller-rig

In the last graphic (Fig. 6 (b)), the stability of the system is shown in terms of lateral displacement y_{disp}. It is interesting to note that the controller is able to locally maintain the system in a stable state.

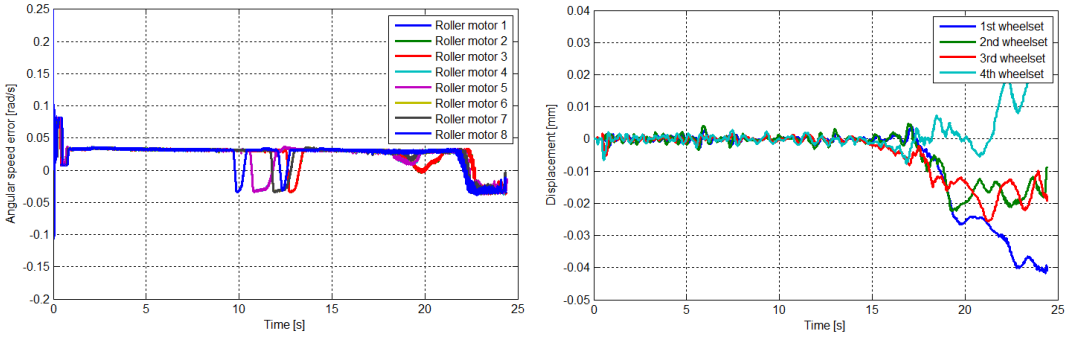

(a) (b)

Figure 6. (a) angular speed error e_ω of the CDSO roller-rig (b) lateral displacement y_{disp} of the CDSO roller-rig

4.2 Numerical simulations

In this section, the authors present the performance and robustness analysis performed on the CDSO HIL system model during braking test of the E464 locomotor under degraded adhesion conditions. The analysis is carried out starting by the nominal conditions and by modifying several HIL system parameters. The robustness analysis on the realistic model of the CDSO HIL system represents a great improvement compared with previous works [5], [8] since most of the system components are widely characterized by the real data. Moreover, the main important issues faced with this work are the controller robustness with respect different working scenarios and the HIL system stability analysis in a model completely 3D.

The robustness analysis is defined perturbing separately different kind of parameters: Constrain parameters (DOF, stiffness and damping, z-position, longitudinal and lateral displacements); Controller parameters (uncertainties in the controller parameters) and Sensor parameters (uncertainties in the sensor parameters).

In the following paragraphs, for reasons of synthesis, only the 1st test is shown with complete results (in terms of torque estimation error e_c and angular speed error e_ω); the other tests are shown in terms of maximum errors.

4.2.1 *Test 1*

The test 1 is referred to the evaluation of the CDSO roller-rig robustness when the 5 DOFs of the fixed and mobile constrained are reduced to 2 DOFs (only the motion in the x-y directions are constrained).
In the presented test, the torque estimation error e_c and the angular speed error e_ω are shown. It is possible to note the robustness of the controller (considering the torque estimation error Fig. 7 (a) and the angular speed one Fig. 7 (b)), able to ensure the stability of the system both during the initial transient (which could be strong) and during the recovery adhesion part.

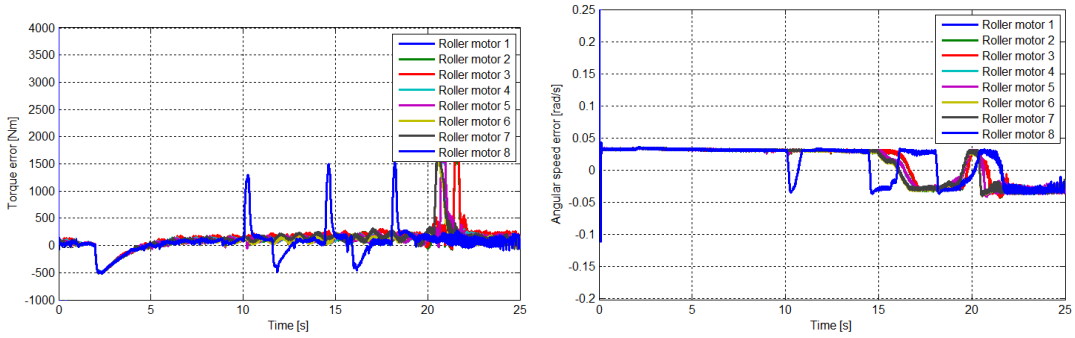

(a) (b)

Figure 7. (a) torque estimation error e_c of the CDSO roller-rig (b) angular speed error e_ω of the CDSO roller-rig

4.3 Other tests

In this section, the results of the other tests performed during the sensitivity analysis can be summarized. The tests are carried out according with the table 2. The results are displayed through the analysis of the maximum values of the torque estimation error e_c, the angular speed error e_ω and the longitudinal x_{disp} and lateral y_{disp} displacements. Analysing the

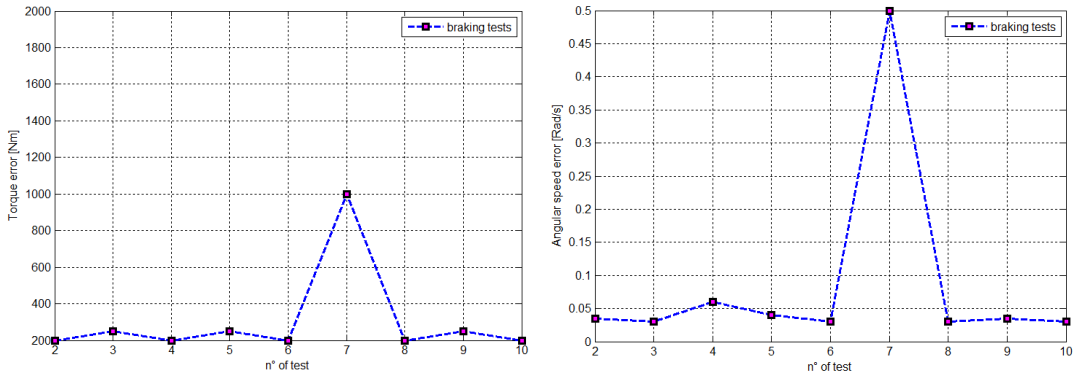

(a) (b)

Figure 8. (a) Torque estimation errors e_c of the CDSO roller-rig (b) Angular speed errors e_ω of the CDSO roller-rig

behaviour of the angular speed error e_ω and of the torque estimation error e_c (Fig. 8 (a)(b)),and also, the trend of the x-displacement x_{disp} and of the y-displacement y_{disp} (Fig. 9 (a)(b)) it is worth noting the high controller robustness and the HIL system stability both for the initial transients and for the recovery adhesion.

5 Conclusions and further developments

In this paper, the authors presented an accurate and realistic model of the innovative HIL roller-rig installed in the "Centro di Dinamica Sperimentale Firenze-Osmannoro" (CDSO). This HIL system represents (according with the state of art of fullscale roller-rigs) one of the most innovative test-rig to simulate degraded adhesion conditions, by means of the

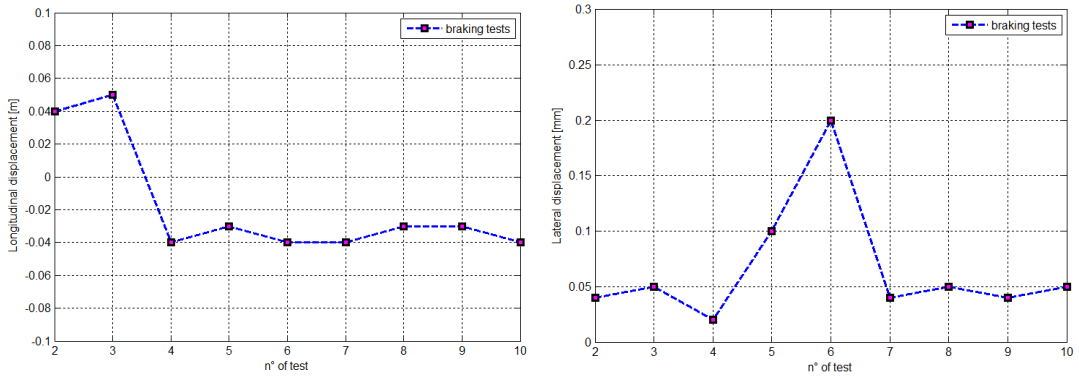

(a) (b)

Figure 9. (a) Longitudinal displacements x_{disp} of the CDSO roller-rig (b) Lateral displacements y_{disp} of the CDSO roller-rig

innovative control architecture. This work has been developed in collaboration with Italcertifer, the owner of the CDSO test-rig, which has provided the technical documentations both of the HIL system and of the E464 locomotor (this vehicle will be tested on the CDSO roller-rig in the first testing activities). In this paper the authors, in collaboration with Trenitalia and Italcertifer, have evaluated several critical conditions for the CDSO roller-rig when operative conditions are not the same of the nominal cases (see Table 2 for a detailed description of the evaluated cases), and, through the complete 3D model of the roller-rig, have performed a performance and robustness analysis. The analysis has showed interesting results in terms of robustness (both of the controller and of the estimation part) and in terms of system stability, as showed by means of the behaviour analysis of the angular speed error e_ω, torque estimation error e_c and displacements x_{disp}-y_{disp}. As regards further developments, the first aim will be the comparison of the obtained model results with the experimental data of the real HIL Osmannoro test rig in order to obtain an experimental validation of the whole model.

References

[1] Iwnicki S., Allen P.D. *Handbook of Railway Vehicle Dynamics*. CRC/Taylor and Francis, UK, 2006.

[2] Rete Ferroviaria Italiana (RFI) *Banco a rulli: relazione tecnica*. Rev. 2.0, 2010.

[3] Trenitalia and Bombardier Transportation *Manuale di manutenzione di secondo livello: locomotore E464*. 2007.

[4] Allotta B., Malvezzi M., Meli E., Pugi L., Ridolfi A., Rindi A., Vettori, G. Simulation of railway braking tests under degraded adhesion conditions. *Proceedings of the International Multibody System Dynamics IMSD 2012*, 2012

[5] Malvezzi M., Allotta B., Pugi,L. Feasibility of degraded adhesion tests in a locomotive roller rig. *Proceedings of the Institution of Mechanical Engineering, Part F*, 2008

[6] Jaschinki A., Chollet H., Iwnicki S. The application of the roller rigs to railway vehicle dynamics. *Vehicle System Dynamics*, Vol. 31, pp. 345-392, 1999.

[7] Malvezzi M., Meli E., Rindi A., Falomi S.Determination of wheel-rail contact points with semianalytic method. *Multibody System Dynamics*, Vol. 20, pp. 327-358, 2012.

[8] Conti R., Meli E., Pugi,L. , Malvezzi,M., Bartolini,F., Allotta,B., Rindi,A., Toni,P. A numerical model of a HIL scaled roller rig for simulation of wheel-rail degraded adhesion condition. *Vehicle System Dynamics*, Volume 50, pp.775-804, 2012.

[9] S. Magheri, M. Malvezzi, E. Meli, A. Rindi. An innovative wheel-rail contact model for multibody applications. *Wear*, 271, 462-471, 2011.